國立臺灣大學醫學院微生物學研究所

碩士論文

Graduate institute of Microbiology

College of Medicine

National Taiwan University

Master Thesis

探討 SMYD3 在同源重組中扮演的角色

Characterization of the Roles of SMYD3 in Homologous Recombination

王品瑀

Pin-Yu Wang

指導教授：鄧述諄 博士

Advisor: Shu-Chun Teng, Ph.D.

中華民國 105 年 7 月

July, 2016

doi:10.6342/NTU201602684

國立臺灣大學（碩）博士學位論文
口試委員會審定書

中文題目：探討 SMYD3 在同源重組中扮演的角色

英文題目：Characterization of the Roles of SMYD3 in Homologous Recombination

本論文係王品瑞君（學號R03445114）在國立臺灣大學微生物學所完成之碩（博）士學位論文，於民國105年7月25日承下列考試委員審查通過及口試及格，特此證明

口試委員：

鄭述謙（簽名）

（指導教授）

李明學

系主任、所長 鄭述謙（簽名）

誌謝

這兩年裡，謝謝鄧述諄老師提供我一個很好的研究環境與在實驗上的指導，還有每次 seminar 前教我如何做一個好的報告者，讓我受益良多。也感謝李財坤老師與李明學老師在每次的 committee 中給予的建議與指導，讓我的碩士論文更趨完整。

謝謝實驗室裡同學與學長姐在實驗中的幫忙、包容與陪伴，尤其是振輝、韻茹和 Cooper 常常提供我方法解決實驗中遇到的問題。也謝謝雅嵐除了與我分享實驗技巧外，也會與我分享生活中的經驗。

這兩年中，尤其謝謝家人對我的支持與包容，還有許多人在這過程中給予我幫助與陪伴，恕我無法一一列舉。希望實驗室的大家，天天都能有好 data，大家都能順利畢業！

doi:10.6342/NTU201602684

中文摘要

SMYD3 在腫瘤形成中為常見的致癌基因。癌症中，過度表現的 SMYD3 與細胞增殖和較差的預後有關聯。在這篇研究中，我們發現 SMYD3 會調控 DNA 修復。在 microarray 和 ChIP-seq 結果顯示 SMYD3 會活化 *MDC1*、*EXO1* 和 *RAD54B* 等與同源重組相關的基因表現。SMYD3 的缺乏會使細胞對 DNA 損傷較敏感，而且同源重組的修復機制也會產生缺陷。在缺乏 SMYD3 的細胞中γ-H2A.X foci 存在的時間延長，而 MDC1 與 BRCA1 foci 的形成減少。而且，當 SMYD3 被抑制時，在 *MDC1*、 *EXO1* 和 *RAD54B* 啟動子處 H3K4me3 的量也會跟著減少。總結，我們發現 SMYD3 藉由調控 *MDC1*、 *EXO1* 和 *RAD54B* 的表現進而影響同源重組修復的能力。

關鍵字：SMYD3、同源重組、DNA 修復

doi:10.6342/NTU201602684

ABSTRACT

SMYD3 emerges as a common oncogene in tumorigenesis, and overexpression of SMYD3 is linked to increased cell proliferation and poor prognosis in human cancers. Here we show that SMYD3 regulates DNA repair. ChIP-seq and microarray analyses demonstrate that SMYD3 binds and activates homologous recombination genes (*MDC1*, *EXO1*, and *RAD54B*) in MCF7 cells. SMYD3-depleted cells became hypersensitive to DNA damage and were defective in homologous recombination repair. Retention of γ-H2A.X foci and decrease of MDC1 and BRCA1 foci were observed in SMYD3 knockdown cells. Moreover, depletion of SMYD3 inhibited H3K4 trimethylation on *MDC1*, *EXO1*, and *RAD54B* promoter. Together, we discover a novel mechanism of SMYD3 in homologous recombination by regulating the expression of *MDC1*, *EXO1*, and *RAD54B*.

doi:10.6342/NTU201602684

CONTENTS

doi:10.6342/NTU201602684

Chapter 1 Introduction

Cancer development is related to aberrant pattern of histone modification which causes abnormal genes expression. Many histone methyltransferases have been implicated in cancer aggressiveness (Albert and Helin, 2010; Cebria et al., 2002; Panier and Boulton, 2014), one of which is SMYD3 (SET and MYND domain containing protein 3). SMYD3 is highly expressed in colorectal carcinomas, hepatocellular carcinomas, pancreatic cancer, prostate cancer and breast cancer (Hamamoto et al., 2004; Hamamoto et al., 2006). SMYD3 regulates genes transcription through methylating histones, including H3K4me2/3 (Martin and Zhang, 2005), H4K20me2/3 (Foreman et al., 2011) and H4K5me1/2/3 (Van Aller et al., 2012). For example, SMYD3 upregulates *MMP9* (Cock-Rada et al., 2012) and *hTERT (Liu et al., 2007)* directly by SMYD3-mediated trimethylation of H3K4. SMYD3 also methylates non-histone proteins. VEGFR (Kunizaki et al., 2007), a receptor tyrosine kinase, is methylated by SMYD3 at lysine 831 to enhance its activity, which promotes invasion and metastasis ability in cancer development. Moreover, SMYD3 methylates MAP3K2 (Mazur et al., 2014) at lysine 260 to activate Ras/Raf/MEK/ERK signaling by inhibiting binding of PP2A phosphatase complex to MAP3K2. SMYD3 mainly locates in cytoplasm at G0/G1 phases and moves to nucleus at S/G2 phases (Hamamoto et al., 2004). Above evidences indicate the mechanism of SMYD3-mediated oncogenesis in the nucleus and cytoplasm.

DNA doubles-strand breaks (DSBs) that are not properly repaired will result in cell death and genomic instability. DSBs are mainly repaired by non-homologous end

doi:10.6342/NTU201602684

joining (NHEJ) or homologous recombination (HR). NHEJ ligates DNA breaks directly by DNA ligase IV throughout the cell cycle, but is most important during G1 when homologous template for recombination is unavailable; HR occurs predominantly in S and G2 phases when a sister chromatid is accessible (Symington and Gautier, 2011). Therefore, HR repair is important for hyper-proliferation cells, like cancer cells, to overcome DNA damages such as DNA double strand breaks and arrested replication forks to maintain genome integrity (Bishop and Schiestl, 2002).

DNA double strand breaks (DSBs) are initially sensed by MRN complex (Mre11-Rad50-Nbs1) followed by recruitment of ATM and MDC1. ATM phosphorylated H2A.X (γ-H2A.X) are subsequently recognized by MDC1 (Stucki et al., 2005). Interaction between MDC1 and ATM through FHA domain further contributes to the extension of γ-H2A.X around the DNA DSBs (Huen and Chen, 2008). MDC1 also mediates retention of MRN complex (Chapman and Jackson, 2008) and acts as a platform for accumulation of BRCA1 (Zhenkun Lou et al., 2003a) and 53BP1 (Bekker-Jensen et al., 2005) at DSBs. In the initiation of HR repair, MRN complex and CtIP conduct 5'-to-3' short-range DNA end resection to generate 3' single-stranded DNA (ssDNA) (Sartori et al., 2007). The subsequent long-range resection is conducted by a nuclease, EXO1 (Tran et al., 2004), and BLM, a helicase (Nimonkar AV, 2008). The exposed ssDNA is immediately bound by RPA to prevent the formation of secondary structure. RPA is then displaced by Rad51, a recombinase, and RAD51-ssDNA filaments form with the help of BRCA2 (Thorslund et al., 2010). Working in concert with RAD51-ssDNA filaments, RAD54B, a DNA-dependent ATPase, drives the search for a homologous template and strand invasion (Mason et al., 2015). After pairing with complementary DNA sequence and forming a D-Loop, the undamaged homologous

doi:10.6342/NTU201602684

DNA sequence is used as a template for intact DNA synthesis to resolve DNA damages.

HR repair pathway is regulated by the recruitment of DNA repair proteins and many posttranscriptional modifications of proteins (phosphorylation, ubiquitylation, sumoylation, and methylation) (Heyer et al., 2010). Histone posttranscriptional modifications have been indicated to orchestrate dynamics of DNA damage repair proteins (Hunt et al., 2013). Shortly, after DNA damage occurring, H2A.X is phosphorylated by ATM or ATR immediately and interacts with MDC1. MDC1 then recruits RNF8 (Mailand et al., 2007) and RNF168 (Mattiroli et al., 2012) to catalyze K63-ubiquitilation on H2A and H2A.X which mediate the recruitment of BRCA1 and 53BP1 for HR and NHEJ, respectively. Nowadays, the posttranscriptional modification of proteins in HR has been studied a lot. However, the evidence of transcriptional regulation of HR genes is insufficient.

Most studies have focused on the ability of SMYD3 to promote cell proliferation and metastasis through methylating histones to activate gene expression and/or directly methylating target proteins to enhance its activity. Interestingly, there is significant correlation between SMYD3 and homologous recombination (HR) repair pathway in our microarray and ChIP-seq data. The mRNA of *MDC1*, *EXO1*, and *RAD54B*, which are HR associated genes, decreased after inhibition of SMYD3 in MCF7 cells. In addition, SMYD3 localizes to these genes in ChIP-seq analysis. Therefore, we proposed that SMYD3 regulates *MDC1*, *EXO1*, and *RAD54B* epigenetically to affect the efficiency of homologous recombination. In our results, depletion of SMYD3 caused DNA-damage hypersensitivity and decreased homologous recombination activity. These defects could result from diminished expression of *MDC1*, *EXO1*, and *RAD54B*. In

doi:10.6342/NTU201602684

addition, the H3K4me3, one of SMYD3 catalyzed histones, on these genes promoter decreased after suppression of SMYD3. Conclusively, these results suggest that SMYD3 coordinates homologous recombination through regulating expression of *MDC1*, *EXO1*, and *RAD54B*.

doi:10.6342/NTU201602684

Chapter 2 Results

2.1 Loss of SMYD3 results in decreased expression of DNA repair genes

Overexpression of SMYD3 is able to promote cancer cells proliferation and metastasis. To explore novel roles of SMYD3, we analyzed microarray and ChIP-seq data base. The gene expression levels of 264 transcripts were decreased in SMYD3 knockdown MCF7 cells. Moreover, results of ChIP-seq showed that SMYD3 was recruited to 3437 DNA sequences (Supplementary Figure 1). Comparing these two data sets, 28 genes were implicitly regulated by SMYD3. When classified by gene ontology (GO) terms, these genes were highly associated with DNA repair, especially the homologous recombination (HR) repair. To confirm the results from these databases, the expression of *MDC1, EXO1,* and *RAD54B,* which are essential to HR repair (Mason et al., 2015; Tomimatsu et al., 2014; Zhang et al., 2005), were assessed in SMYD3-depleted MCF7 cell. For stable knockdown of SMYD3, a lentivirus shRNA infection system (shSMYD3#1 and shSMYD3#2) was used. We found that the mRNA expression and protein levels of *MDC1* and *EXO1* were significantly reduced after inhibition of SMYD3. Although the protein level of *RAD54B* was not affected, its mRNA expression was also significantly reduced in SMYD3-depleted cells (Figure 1). These results suggest that SMYD3 may be involved in HR repair.

doi:10.6342/NTU201602684

2.2 SMYD3 plays a role in homologous recombination repair

In our results, SMYD3 was able to regulate expression of HR associated genes, including *MDC1*, *EXO1*, and *RAD54B*. In order to know whether SMYD3 plays a role in HR repair, MCF7 DR-GFP cells were used to evaluate homologous recombination activity. Chromosome of DR-GFP cells is inserted with a cassette that contains two differentially mutated *GFP* genes oriented as direct repeats and is separated by a drug selection marker, the puromycin N-acetyltransferase gene (Pierce et al., 1999) (Figure 2). One of the mutant *GFP* genes (with 22 nucleotides deletion) contains I-SceI endonuclease cutting sites, and the other *GFP* gene acts as a donor of WT GFP sequence for homologous recombination. Therefore, the DSBs are created by expressing I-SceI endonuclease in MCF7 DR-GFP cells. The GFP protein is expressed only when the DSBs on *GFP* are repaired by HR.

After knockdown of SMYD3 for three days, MCF7 DR-GFP cells were transfected with pCβASce to express I-SceI endonuclease and generate DSBs. After expressing I-SceI endonuclease for 48 h, MCF7 DR-GFP cells were analyzed by flow cytometry and GFP-positive cells were quantified. Results showed that after depletion of SMYD3, the percentage of GFP-positive cells were significantly reduced (Figure 3) implicating the impairment of homologous recombination in SMYD3-depleted cells. The HR activity assay was performed in U2OS DR-GFP cells in the same way. The HR activity is also defective in SMYD3-depleted U2OS DR-GFP cells (Figure 4). On the other hand,

doi:10.6342/NTU201602684

NHEJ efficiency is negligibly affected by inhibition of SMYD3 (Figure 5). These results suggest that SMYD3 plays an important role in HR repair.

2.3 Inhibition of SMYD3 postpones the DNA repair

To study the DNA damage response after depletion of SMYD3, MCF7 cells were treated with ionizing radiation (IR) (1.67 Gy). The DNA repair kinetics were measured by the accumulation of γ-H2A.X foci, a DNA damages marker (Podhorecka et al., 2010). After treatment with IR, cells were analyzed in different recovery time (1, 2, 4, 24, 48 and 72 h). Compared with shLuc cells, the percentage of γ-H2A.X foci was not different from 1 h to 4 h post-irradiation (Figure 6A). However, percentage of γ-H2A.X foci remained high in SMYD3 knockdown cells after 24 h, implicating that DNA repair was impaired in SMYD3-depleted cells (Figure 6B and 6C). To assess whether the IR sensitivity was affected by inhibition of SMYD3, colony formation assay was performed. After knockdown of SMYD3 for 5 days, cells were treated in different dosages of IR (0, 0.84, 1.67, 3.33 Gy). Colonies were counted at day 15 post-irradiation. Compared to shLuc cells, only one of SMYD3 knockdown clone (shSMYD3#1) showed more sensitivity to IR (Figure 6D). It might due to the deficiency of SMYD3 is strongly deleterious to MCF7 cells that led to few colony formation in SMYD3-knockdown cells even in IR-free groups (Cock-Rada et al., 2012; Hamamoto et al., 2004), or the colonies were too small to be counted in SMYD3-knockdown cells. These results imply that SMYD3 plays a pivotal role in cell proliferation and is required for efficient DNA repair.

doi:10.6342/NTU201602684

2.4 Loss of SMYD3 impairs formation of BRCA1 foci through regulating expression of MDC1

Knockdown of SMYD3 reduced the expression of *MDC1*, *EXO1*, and *RAD54B* (Figure 1). MDC1 is a crucial regulator in DNA repair (Stucki and Jackson, 2004) and participates in the initial recruitment of 53BP1 and BRCA1 (Kolas NK et al., 2007; Minter-Dykhouse et al., 2008; Shi et al., 2008; Wilson and Stern, 2008; Zhenkun Lou et al., 2003b). The accumulation of 53BP1 at DSBs stimulates NHEJ whereas the accumulation of BRCA1 promotes DNA end resection and HR (Escribano-Diaz et al., 2013). To gain further insight into how SMYD3 regulates HR activity, we investigated the formation of BRCA1 foci following exposure to ionizing radiation (IR) in MCF7 cells by immunofluorescence staining. MCF7 cells were treated with IR (1.67 Gy) and recovered at 37℃ for 1hr. Results showed that the MDC1 and BRCA1 foci were diminished in SMYD3-depleted cells after IR-induced DSBs (Figure 7 and 8), which was consistent with lower HR activity in SMYD3-depleted cells. In agreement with the results of NHEJ assay, the recruitment of 53BP1 foci was not affected by depletion of SMYD3. These results indicate that SMYD3 deficiency impairs HR through downregulation of MDC1 and leads to less accumulation of BRCA1 foci at DSBs.

doi:10.6342/NTU201602684

2.5 The establishment of H3K4 trimethylation on HR genes promoter is SMYD3-dependent

SMYD3 was reported primarily to catalyze H3K4 trimethylation (H3K4me3) on promoter region to activate its target genes. To investigate whether inhibition of SMYD3 alters the H3K4me3 patterns on *MDC1*, *EXO1*, and *RAD54B* promoters, the levels of H3K4me3 were evaluated by chromatin immunoprecipitation (ChIP). The primers encompassing the SMYD3-binding sites in ChIP-seq and the TATA-box, a binding site for RNA polII, were used for real-time PCR. Results showed that occupation of H3K4me3 was abolished on the *MDC1*, *EXO1*, and *RAD54B* TATA-box upon depletion of SMYD3 (Figure 9), which suggests that the recruitment of H3K4me3 on these genes promoter relies on SMYD3. Notably, the SMYD3-binding site in ChIP-seq on *MDC1* is near by the TATA box. These results indicate that SMYD3 regulates *MDC1*, *EXO1*, and *RAD54B* through the establishment of H3K4me3 on promoter region.

doi:10.6342/NTU201602684

Chapter 3 Discussion

In this study, we elucidated a novel function of SMYD3 in homologous recombination. Deficiency of SMYD3 reduced the expression of HR associated genes, induced DNA-damage hypersensitive, decreased the level of MDC1 and BRCA1 foci, and led to impairment of homologous recombination. Furthermore, the active transcription marker H3K4me3 on *MDC1*, *EXO1*, and *RAD54B* promoter is SMYD3-dependent. Here, we provide an evidence insight into the transcriptional3 regulation of HR genes relying on SMYD3.

Previous reports have shown that the recruitment of BRCA1 and 53BP1 are mediated by MDC1 (Minter-Dykhouse et al., 2008; Zhenkun Lou et al., 2003b). Here, we found that HR activity and the formation of BRCA1 foci were suppressed in SMYD3-depleted cells. However, the formation of 53BP1 foci was not affected in our experiments (Figure 8). The initial 53BP1 recruitment is mediated by MRN complex, and MDC1 plays a role in sustaining the 53BP1 binding. In MDC1 knockdown cells, 53BP1 foci form normally after IR treatment but disappear rapidly in 2 hours (Bekker-Jensen et al., 2005). In our experiments, BRCA1 and 53BP1 foci were measured at 1 h post-irradiation. Therefore, the reduction of 53BP1 foci was not observed in our results.

SMYD3 knockdown impaired the formation of BRCA1 foci. We further investigate whether it was resulted from the change of mRNA and protein expression of *BRCA1 per se* or affected by the reduction of MDC1. We observed that the mRNA and protein level of *BRCA1* diminished in SMYD3-depleted cells (Figure 10A and 10B). Intriguingly, in

doi:10.6342/NTU201602684

our microarray data, the expression of *BARD1* (BRCA1-Associated RING Domain-1) reduced in SMYD3-depleted cells (Figure 10A). BARD1 and BRCA1 form heterodimer in DNA repair. The interaction with BARD1 increases the E3 ligase activity and the stability of BRCA1 (Choudhury et al., 2004). In our data, MDC1-depleted cells showed decreased BRCA1 foci/protein expression as well (Figure 10C and 10D). Therefore, we assumed the reduction of BRCA1 in SMYD3-depleted cells might due to the downregulation of *BARD1* and *MDC1*.

SMYD3 has different functions in the nucleus and cytoplasm, the amounts of SMYD3 in the nucleus is less than the cytoplasm. To assess whether DSBs induce translocation of SMYD3 into nucleus to activate HR genes transcription, we used nuclear/cytosol fractionation assay to evaluate the changes of SMYD3 in nucleus and cytoplasm after IR treatment (Figure 11). However, the amounts of SMYD3 did not change after IR treatment, which might be due to the limited level of nuclear SMYD3 was sufficient to activate HR genes. We also observed that the expression of *MDC1*, *EXO1*, and *RAD54B* were not changed after IR treatment. Thus, SMYD3 may modulate the constitutive expression of *MDC1*, *EXO1,* and *RAD54B.*

In conclusion, our results demonstrate that *MDC1, EXO1* and *RAD54B* are new target genes of SMYD3 besides *WNT10B (Hamamoto et al., 2006), NKX2.8, MMP9, cMET (Zou et al., 2009), hTERT,* and *CCNA1*. In addition, SMYD3 is linked to DNA repair for the first time. Two ways of SMYD3 to regulate genes expression have been proposed (Robert J. Sims 3rd and Reinberg, 2004). SMYD3-mediated histones methylation could recruit other factors to its binding sites, or SMYD3 associates with RNA PolII to generate broader region of H3K4 methylation. Moreover, previous studies showed that

doi:10.6342/NTU201602684

SMYD3 regulates genes expression with transcription factors. For example, SMYD3 regulates ER-mediated target genes by directly interacting with estrogen receptor which allows localization of SMYD3 to ER target genes and methylates H3K4 on these genes promoter (Kim et al., 2009). SMYD3 also regulates genes involved in cell proliferation and invasion collaborating with PC4 (positive coactivator 4) (Kim et al., 2015). We analyzed the promoter regions of *MDC1*, *EXO1*, and *RAD54B* by PRMO (Dome`nec Farre´ et al., 2003), the consensus binding sequences of C/EBPβ, glucocorticoid receptor, YY1, estrogen receptor, TFIID and XBP-1 were indicated. In the future, we will investigate if SMYD3 regulates the expression of *MDC1*, *EXO1*, and *RAD54B* with these potential transcription factors.

doi:10.6342/NTU201602684

Chapter 4 Materials and methods

4.1 Cell culture and genes knockdown

The breast cancer cell lines MCF7 cells were maintained in DMEM containing 10% FBS, non-essential amino acids (HyClone), sodium pyruvate (HyClone), and antibiotics (HyClone). For the depletion of SMYD3, HEK293T cells for virus packaging were co-transfected with packaging plasmid (pCMV-Δ8.91), envelope (pMDG), and hairpin pLKO-RNAi vectors (National RNAi Core Facility, Institute of Molecular Biology / Genomic Research Centre, Academia Sinica, Taiwan, ROC) to produce lentivirus particles. The oligo sequences of shSMYD3#1/#2 are CCGGGCTTCCCGATATCAACATCTACTCGAGTAGATGTTGATATCGGGAAGCT TTTTG and CCGGCAACTC TTTCACCATCTGTAACTCGAGTTACAGATGGTGAA AGAGTTGTTTTTG, respectively. Virus-containing supernatants were collected at 48 h post-transfection. The cells were treated with virus and polybrene (8 μg/ml) containing medium for 16hr. The transduced cells were selected with puromycin (1 μg/ml) for 5 days.

4.2 Immunoblotting and antibodies

Cells were washed with phosphate-buffered saline (PBS) once in 6-cm dish, then lysed by RIPA buffer (50mM Tris-HCl, 150mM NaCl, 1% NP-40, 0.25% DOC, 1% SDS, 1mM DTT, protease inhibitor, 1mM PMSF, and 1mM EDTA) with protease inhibitor. Cells lysates were separated by SDS-PAGE, transferred to polyvinylidene

doi:10.6342/NTU201602684

difluoride (PVDF) membrane with a 0.22-μm pore size (Immobilon PSQ, Millipore), and blocked overnight with 5% milk in TBS-T (Tris-buffered saline with 0.1% Tween-20) at 4°C. The primary antibodies were SMYD3 (GeneTex), MDC1 (Bethyl), EXO1 (GeneTex), RAD54B (GeneTex), Tubulin (GenTex) and nuclear matrix protein p84 (Novus).

4.3 RNA purification and quantitative reverse transcription PCR

Total RNA was isolated using the RNeasy kit (Qiagen). RNA was reverse-transcribed into first-strand cDNA using Maxima First Strand cDNA Synthesis Kit, with DNase (Thermo). cDNA was amplified with KAPA SYBR fast PCR mix (Kapa Biosystems, Woburn, MA) and subjected to analysis using a *CFX Connect* Real Time System thermal cycler (Bio-Rad). Q-PCR for *RPL30* mRNA (which encodes the ribosomal protein L30) was used as an internal control. The relative abundance of mRNA was calculated after normalization with *RPL30* mRNA using the CT equation.

4.4 Homologous recombination assay

MCF7 DR-GFP and U2OS DR-GFP stable cells (provided by Dr. Hung-Yuan, Chi's lab) possess two differentially mutated *GFP* genes oriented as direct repeats and separated by a drug selection marker, the puromycin N-acetyltransferase gene (Pierce et al., 1999). One of the mutated *GFP* genes contains recognizing site for I-SceI endonuclease and gene deletion. After knockdown of SMYD3 for three days, MCF7

doi:10.6342/NTU201602684

DR-GFP and U2OS DR-GFP stable cells were transfected with pCβASce to express I-SceI which induces double strand breaks on *GFP*. After 48 hours, GFP-positive cells were measured by flow cytometry (FACSCalibur). Ds-Red was transfected as transfection efficiency control.

4.5 Plasmid end-joining assay

Plasmid End-joining assay was conducted as previous described (Shun-Fu Tseng et al., 2005). pGL3-promoter plasmid (Promega) which harbors a luciferase reporter gene was completely linearized by restriction endonucleases HindIII and confirmed by agarose gel electrophoresis. The linearized DNA was subjected to phenol/chloroform extraction, ethanol-precipitated, and dissolved in sterilized water. Then, the linear luciferase reporter was transfected into MCF7 cells. HindIII cuts at the region between promoter and luciferase gene, the expression of luciferase does not be influenced. Luciferase is expressed when cutting sites are repaired by precise end-joining. The luciferase activity was assayed by Luciferase assay system (Promega). Renilla was used as a control.

4.6 Immunofluorescence staining

MCF7/shSMYD3-MCF7 cells were cultured on coverslips two days followed by ionizing radiation (IR) treatment (~3 Gy/min, IBL 637, CIS Bio International, Saclay, France). Then, Cells were fixed by 4% paraformaldehyde and cell membrane was permeabilized with 0.1% Triton-X in PBS for 10 min. After washed three times in PBS,

doi:10.6342/NTU201602684

coverslips were blocked with 1% BSA in PBS and incubated at room temperature with primary antibody (γ–H2AX (Millipore, Upstate), BRCA1 (Santa Cruz), MDC1 (Bethyl) and 53BP1 (Santa Cruz)) for 3 hr. After three times washed in PBS containing 0.05% Triton-X for 5 min, cells were incubated with secondary antibody for another 1 hr. Finally, coverslips were washed three times with PBS containing 0.05% Triton-X and embedded in DAPI (1 ug/ml) containing mounting solution (DAPI: mounting solution = 1:2). Cells with more than 5 foci were counted as positive.

4.7 Colony formation assay

Control (shLuc) or shSMYD3 knockdown MCF7 cells were seeded (5000 cells for shLuc, 10,000 and 20,000 cells for shSMYD3#1 and shSMYD3#2, respectively) in 6-cm dish two days before IR (0, 0.84, 1.67, 3.33 Gy) treatment. After IR treatment, cells were incubated for 15 days. Cells were fixed in 4% paraformaldehyde for 5 min, washed once with PBS, stained with 0.1% crystal violet then washed again with distilled water. The survival rate was calculated by comparing the colonies number with non-irradiated cells in each group.

4.8 Chromatin immunoprecipitation (ChIP)

ChIP assays were performed according to the manufacturer's protocol (Upstate Biotechnology). Briefly, approximately 2×10^6 MCF7 cells or SMYD3-knockdown MCF7 cells were used. The cells were fixed by adding formaldehyde to a final concentration of 1% and incubated for exactly 10 minutes. The cells were washed twice with ice-cold PBS containing protease inhibitors and harvested on ice. The lysates were

doi:10.6342/NTU201602684

sonicated to shear the DNA to fragment lengths of 200 to 500 bps. Complexes were immunoprecipitated overnight with 2 μg of antibodies specific for H3K4me3 or mouse IgG (sc-2025, Santa Cruz). Input samples were processed in parallel. Antibody/protein complexes were collected on 50 μl of protein G-coupled sepharose beads (GE Healthcare) and washed as follows: once with Tris/EDTA-150 mM NaCl, twice with Tris/EDTA-500 mM NaCl and once with PBS. Immune complexes were eluted with 1% SDS and TE buffer. After decrosslinking, DNA was purified using a PCR cleanup kit (Invitrogen) and analysed by qRT-PCR. The results were expressed as the percentage of the initial inputs.

4.9 Nuclear/cytosol fractionation

Approximately 1×10^6 MCF7 cells were used. The cells were trypsinised and washed in ice-cold PBS twice. Cells were lysed on ice for 10 min in 250 ul cytoplasmic lysis buffer (0.1% Triton-X, 10 mM HEPES-KOH pH7.9, 10 mM KCl, 1.5 mM $MgCl_2$, 0.34 M Sucrose, 10% glycerol) containing protease inhibitor, 1 mM DTT, and 10 mM PMSF. Nuclear sediments were collected by centrifugation at 6,000 rpm for 1 min and pellets were washed with 1ml cytoplasmic lysis buffer twice. Nuclei were lysed in RIPA buffer (50 mM Tris-HCl, 150 mM NaCl, 1% NP-40, 0.25% DOC, 1% SDS, 1 mM DTT, protease inhibitor, 1 mM PMSF, 1 mM EDTA) and lysed completely by sonication. Nuclei lysates were separated by SDS-PAGE, transferred to polyvinylidene difluoride (PVDF) membrane with a 0.22-μm pore size (Immobilon PSQ, Millipore), and blocked with 5% milk in TBS-T (Tris-buffered saline with 0.1% Tween-20). Membranes were hybridized in primary antibody overnight at 4℃. The primary antibodies were SMYD3

doi:10.6342/NTU201602684

(GeneTex) and Tubulin (GeneTex).

doi:10.6342/NTU201602684

Chapter 5 Figures

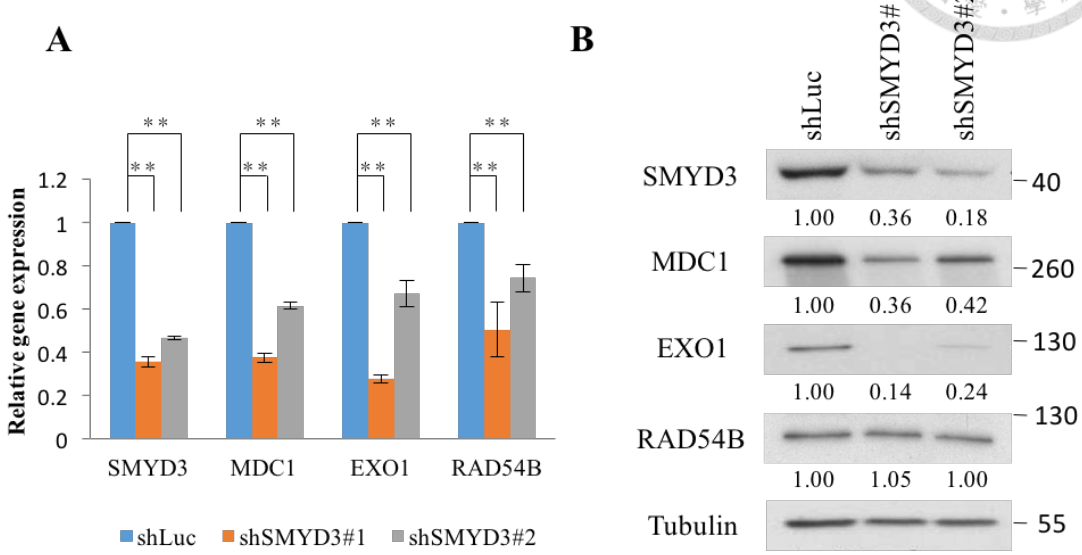

Fig 1. Depletion of SMYD3 influences expression of *MDC1*, *EXO1*, and *RAD54B*. (A) After knockdown of SMYD3 for 5 days, the mRNA of *MDC1*, *EXO1*, and *RAD54B* were analyzed by real–time PCR. RPL32 was used as internal control. The mRNA of *MDC1*, *EXO1*, and *RAD54B* was reduced after inhibition of SMYD3. (B) After knockdown of SMYD3 for 5 days, cells were lysed in RIPA buffer. The protein level of MDC1 and EXO1 in SMYD3-knockdown cells (shSMYD3#1, 2) were decreased. However, the protein level of RAD54B was not diminished after SMYD3 knockdown. Tubulin was used as internal control. Error bar represents the mean ± S.D. **, $p < 0.01$.

doi:10.6342/NTU201602684

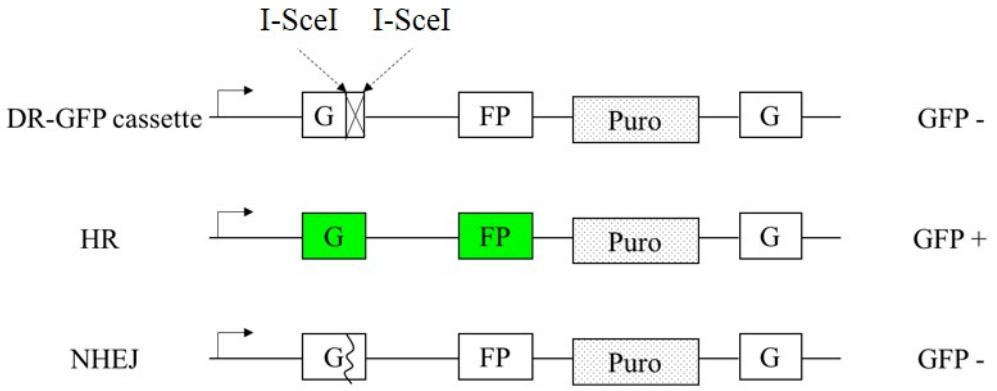

Fig 2. Homologous recombination activity assay. DR-GFP cassette is a recombination substrate for evaluating homologous recombination activity. It is composed of a *GFP* genes with two I-SceI recognizing sites and a wild-type internal *GFP* for homologous pairing which are separated by a puromycin resistant gene. After generation of DSBs by I-SceI, there are two main ways to repair DSBs. One is homologous recombination (HR), the damaged *GFP* uses the wild-type internal *GFP* to synthesis intact *GFP* and the cells express GFP. If DSBs are repaired by non-homologous end joining (NHEJ), the *GFP* gene cut by I-SceI remains mutant because of gene deletion and cells do not express GFP.

doi:10.6342/NTU201602684

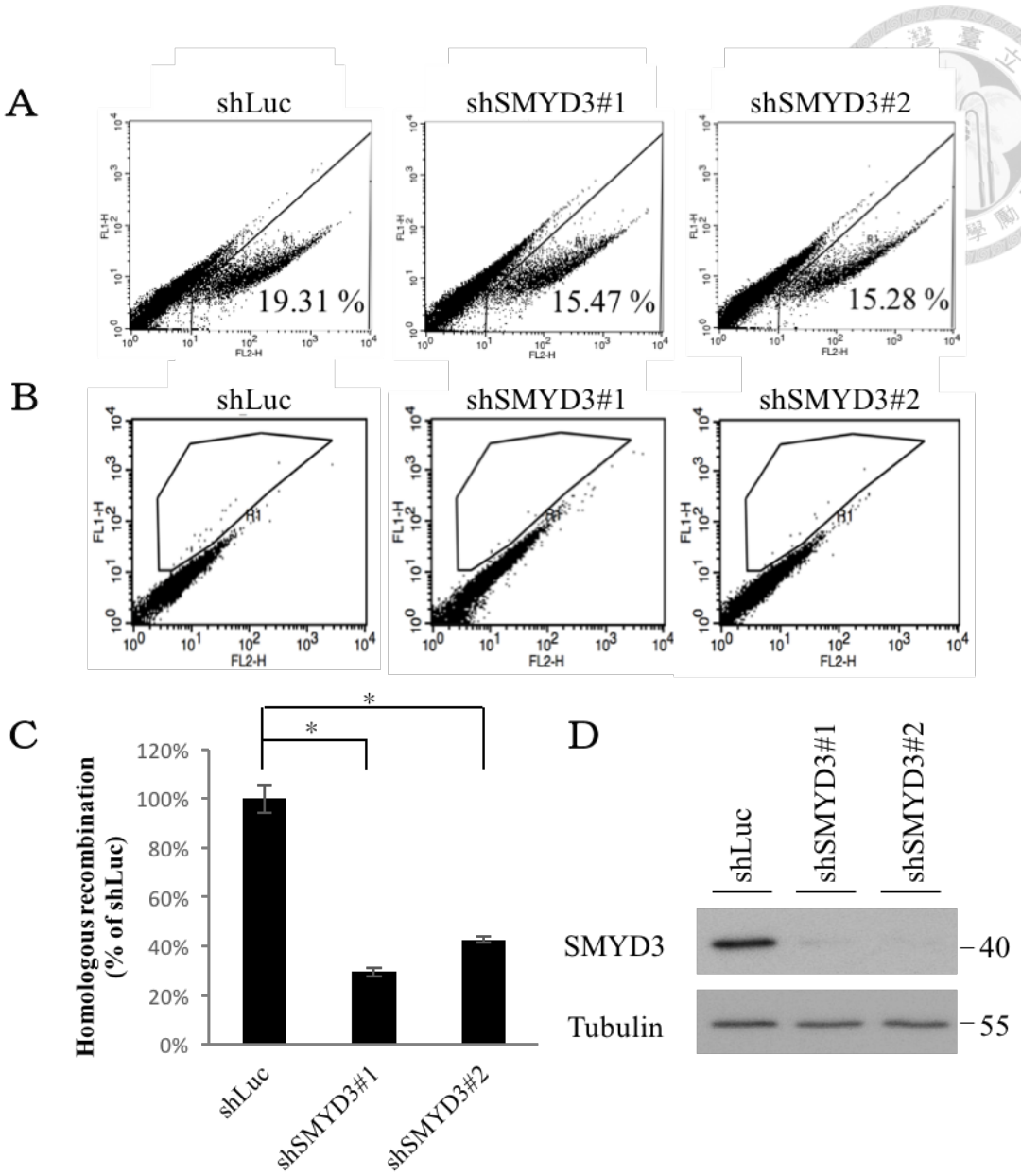

Fig 3. Homologous recombination activity is defective in SMYD3-depleted cells. (A) DS-Red was used as transfection efficiency control in homologous recombination assay. The transfection efficiency was equal in SMYD3 knockdown cells and control. (B) HR efficiency was measured in MCF7 DR-GFP cells after knockdown SMYD3 for 5 days. The cells in circle are quantified as GFP-positive cells. FL1, green fluorescence; FL2, red-orange color. (C) Homologous recombination activity is reduced in SMYD3-depleted cells. Error bar represents the mean ± S.D. *, $p < 0.05$. (D) Western blot shows knockdown efficiency of SMYD3.

doi:10.6342/NTU201602684

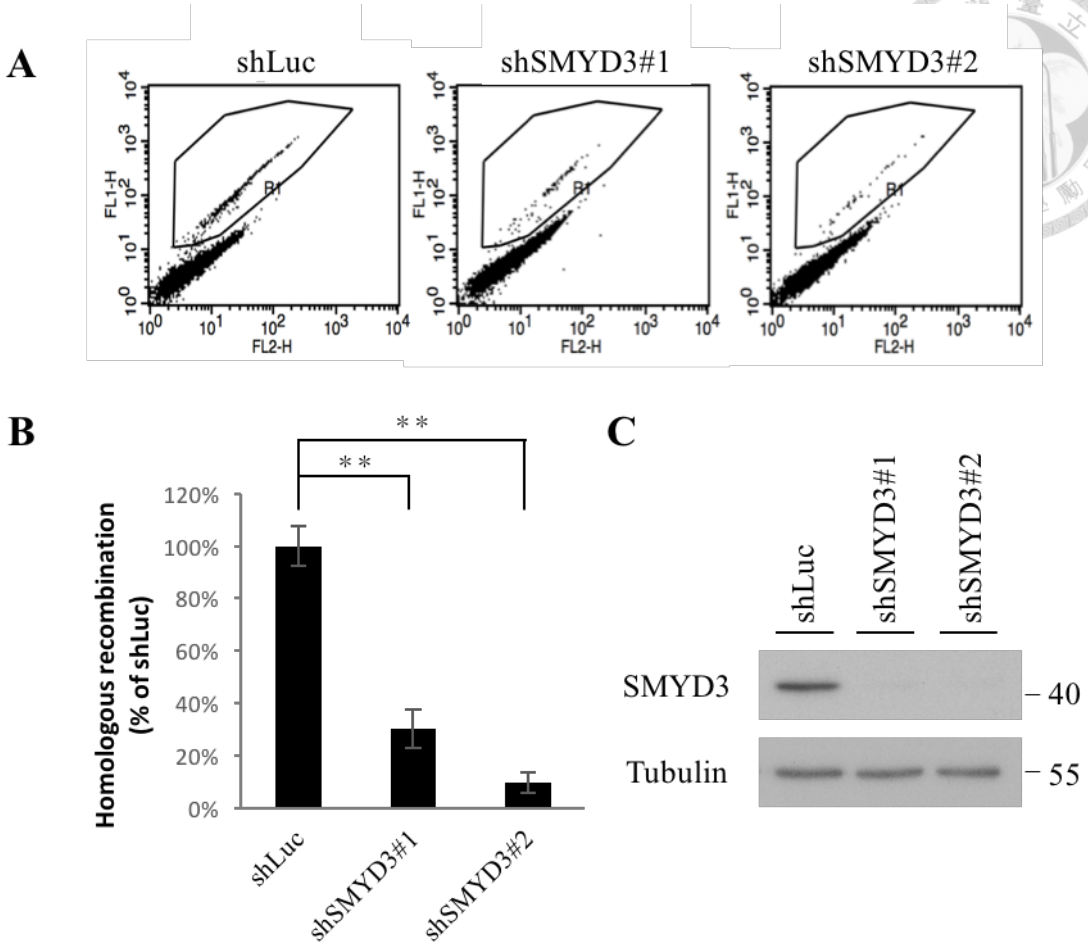

Fig 4. Homologous recombination activity reduced in SMYD3-depleted U2OS cells. (A) HR efficiency was also measured in U2OS DR-GFP cells after SMYD3 knockdown for 5 days. The cells in circle are quantified as GFP-positive cells. FL1, green fluorescence; FL2, red-orange color. (B) Homologous recombination activity is suppressed by depletion of SMYD3. Error bar represents the mean ± S.D. **, $p < 0.01$. (C) Western blot shows knockdown efficiency of SMYD3.

doi:10.6342/NTU201602684

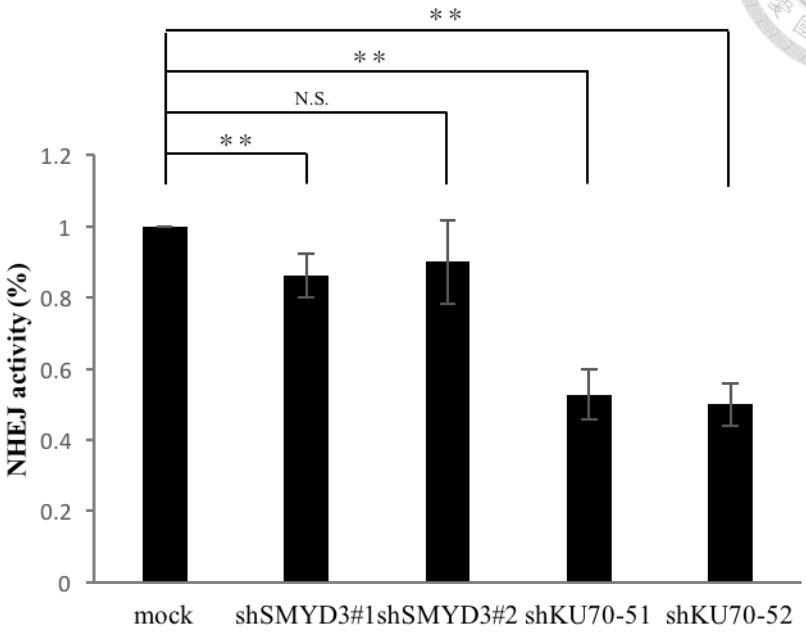

Fig 5. NHEJ is marginal affected by depletion of SMYD3. NHEJ is another mainly DNA repair pathway for DSBs. The NHEJ activity was measured in SMYD3-knockdown and Ku70-knockdown MCF7 cells. The Ku70-knockdown cells were used as the positive control. NHEJ activity was calculated by normalization of luciferase with renilla. After depletion of SMYD3, the NHEJ activity was marginal affected. Error bar represents the mean ± S.D. **, $p < 0.01$; N.S., no significance.

doi:10.6342/NTU201602684

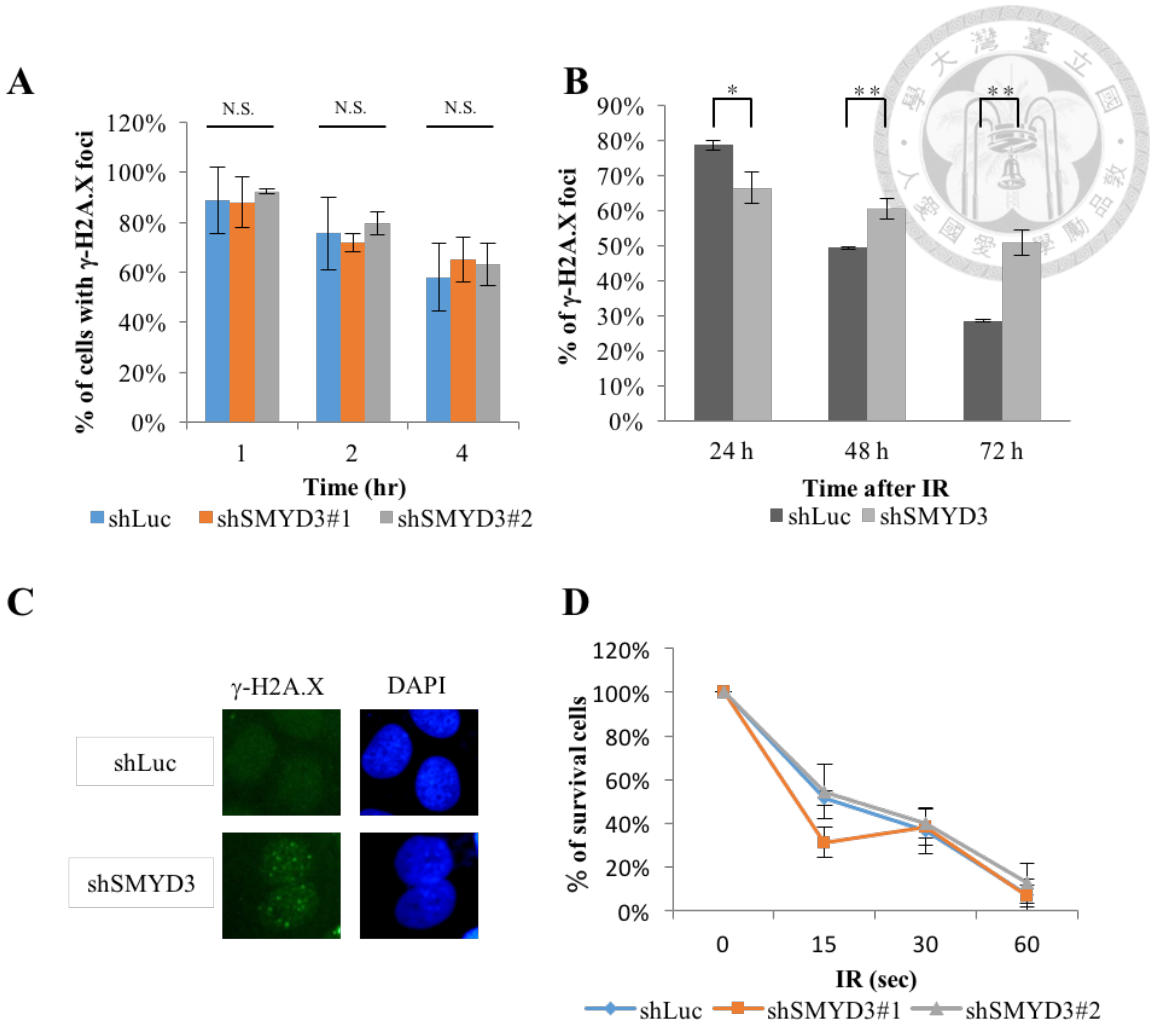

Fig 6. Resolution of DSBs is delayed in SMYD3-depleted cells. After knockdown of SMYD3 for 5 days, MCF7 cells (shLuc and shSMYD3) were treated with IR (1.67 Gy) and fixed for immunofluorescence staining of γ-H2A.X at indicated times. (A) (B) Percentage of γ-H2A.X foci was shown in three independent experiments. 100 nuclei were counted in each experiment. Error bar represents the mean ± S.D. *, $p < 0.05$; **, $p < 0.01$; N.S., no significance. (C) Representative micrographs of γ-H2A.X at 72 h post-irradiation are shown. (D) Cell viability was evaluated by colony formation assay. MCF7 cells stably expressing shRNAs were treated with IR in different dosages. The cells were stained with crystal violet at day 15 post-irradiation. The colonies were counted in three independent experiments. Error bar represents the mean ± S.D.

doi:10.6342/NTU201602684

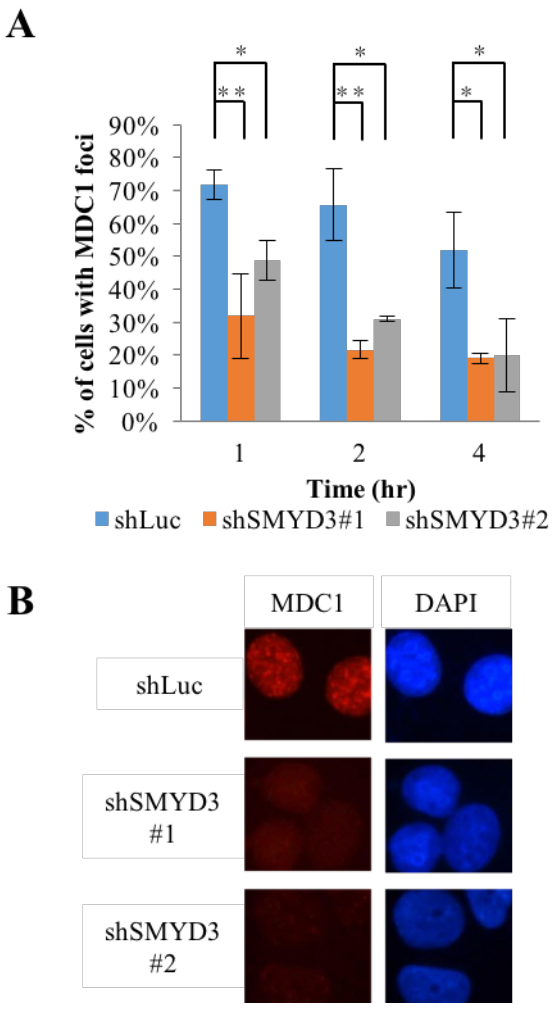

Fig 7. Recruitment of MDC1 is deficient in SMYD3-depleted cells. After knockdown of SMYD3 for 5 days, MCF7 cells (shLuc and shSMYD3) were treated with IR (1.67 Gy) and fixed for immunofluorescence staining of MDC1 at indicated times. (A) Percentage of MDC1 foci was reduced in SMYD3-depleted cells. 100 nuclei were counted in each experiment. Error bar represents the mean ± S.D. *, $p < 0.05$; **, $p < 0.01$. (B) Representative micrographs of MDC1 foci at 1 h post-irradiation are shown.

doi:10.6342/NTU201602684

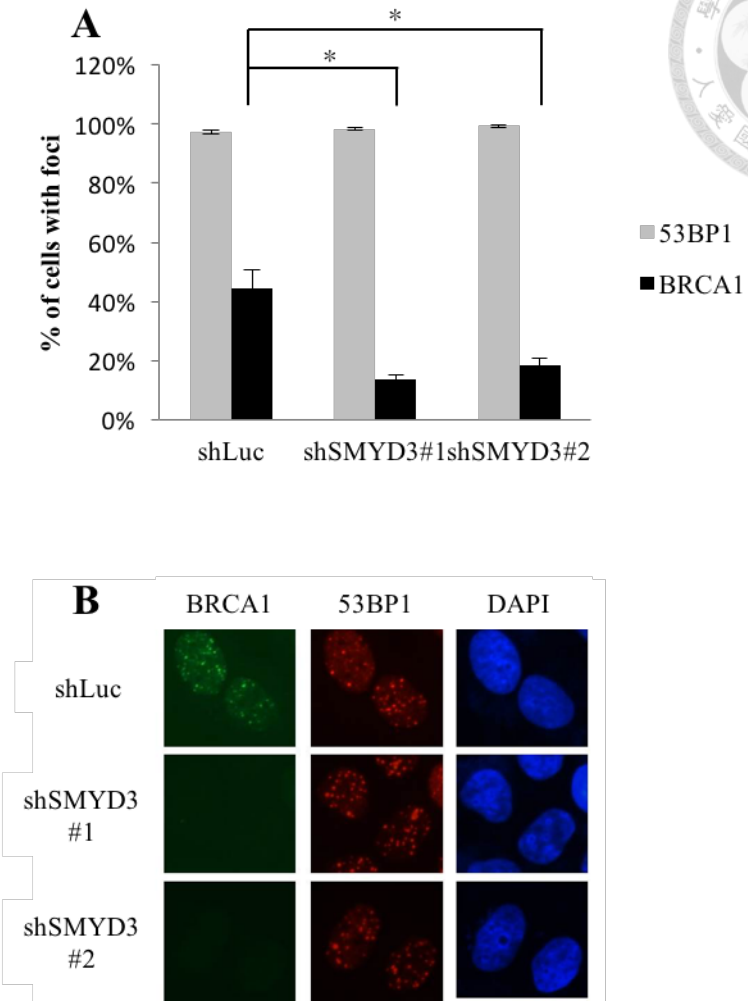

Fig 8. Formation of BRCA1 is deficient in SMYD3-depleted cells. After knockdown of SMYD3 for 5 days, MCF7 cells (shLuc and shSMYD3) were treated with IR (1.67 Gy) and recovered at 37℃ for 1 h. (A) Percentage of cells with BRCA1 foci significantly reduced after inhibition of SMYD3. Nevertheless, the formation of 53BP1 is not affected. 100 nuclei were counted in each experiment. Error bar represents the mean ± S.D. *, $p < 0.05$. (B) Cells were fixed for immunofluorescence staining of BRCA1 and 53BP1.

doi:10.6342/NTU201602684

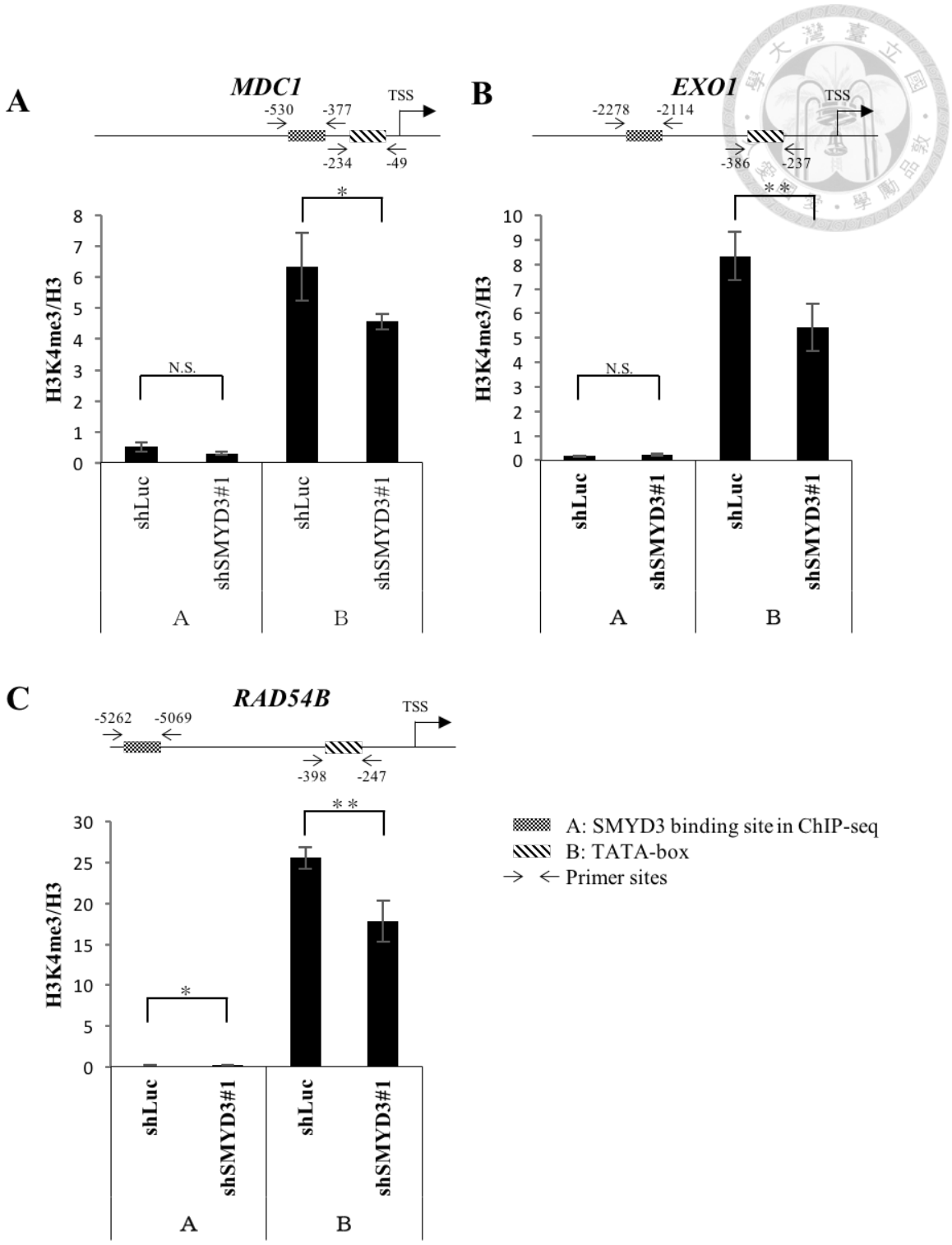

Fig 9. Occupation of H3K4me3 on TATA-box is abrogated in SMYD3-depleted cells. The amount of H3K4me3 on (A) *MDC1*, (B) *EXO1*, and (C) *RAD54B* was assayed by ChIP. A: SMYD3-binding site in ChIP-seq, B: TATA-box. The net amount of H3K4me3 was enriched at region B compared to region A. After depletion of SMYD3,

doi:10.6342/NTU201602684

the H3K4me3 at region B of *MDC1, EXO1* and *RAD54B* decreased. However, the amount of H3K4me3 at region A was not affected by SMYD3 knockdown. The percentage of H3K4me3 in input was normalized with H3. Error bars represent s.e.m. *, $p < 0.05$; **, $p < 0.01$; N.S., no significance.

doi:10.6342/NTU201602684

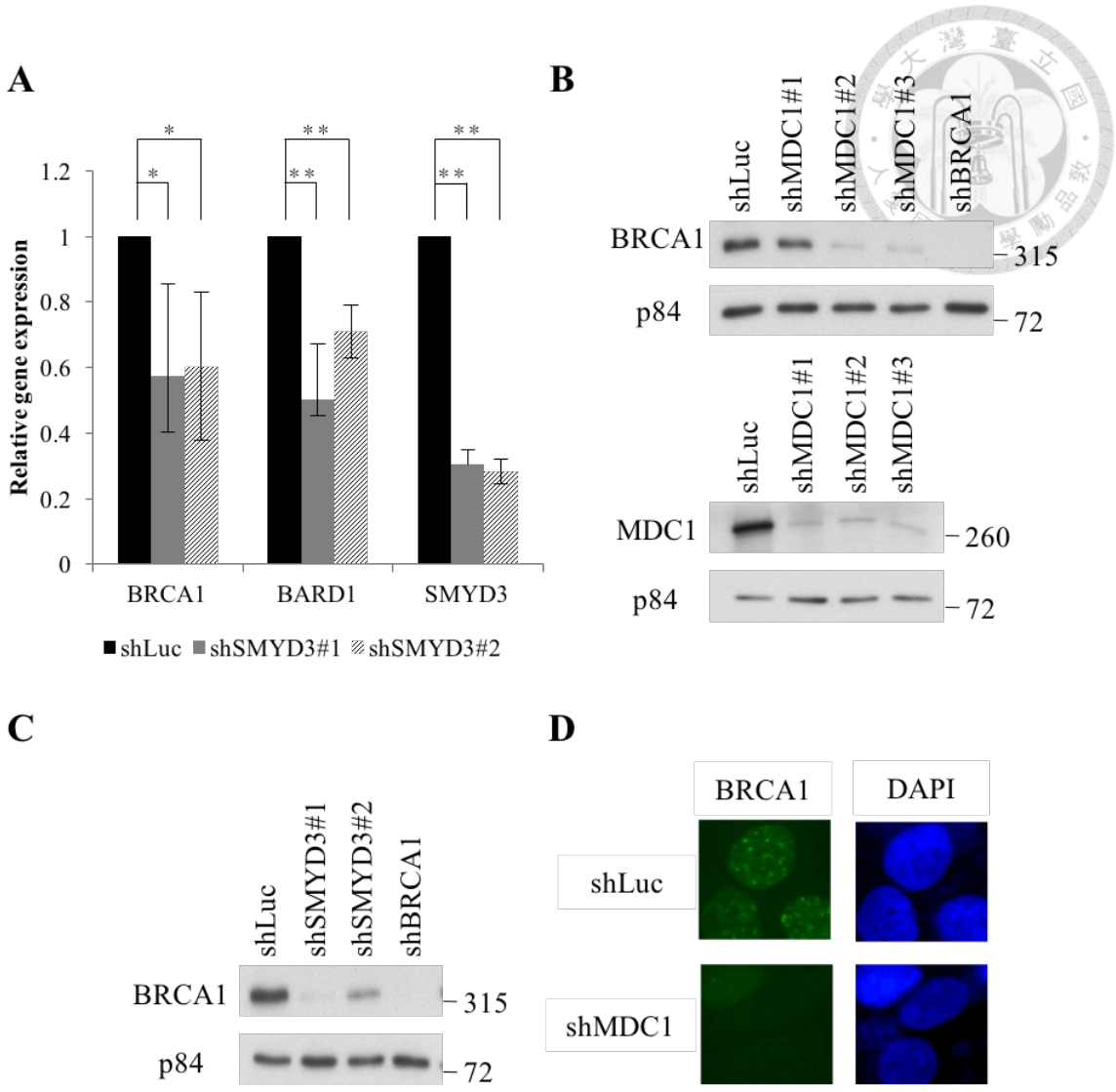

Fig 10. BRCA1 reduces in SMYD3-depleted cells. (A) Expression of *BRCA1* and *BARD1* decreased in SMYD3 knockdown cells. Error bar represents the mean ± S.D. *, p <0.05; **, p <0.01. (B) BRCA1 reduced in three knockdown clones of MDC1. Knockdown efficiency of MDC1 was shown. p84 was used as internal control. (C) BRCA1 reduced in SMYD3-depleted cells. (D) Representative micrographs of BRCA1 in MDC1-depleted cells after IR treatment.

doi:10.6342/NTU201602684

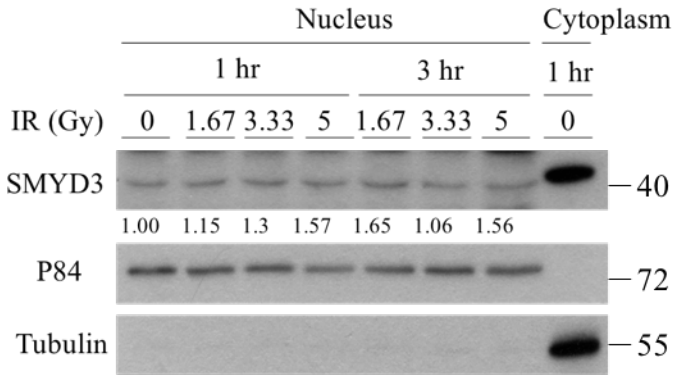

Fig 11. The amount of SMYD3 in nucleus does not influenced after IR. The amount of SMYD3 in nucleus was analyzed by nuclear/cytosol fractionation at 1 h and 3 h post-irradiation with different dosage. Nuclear SMYD3 is less than cytosol SMYD3. After exposure to IR, the distribution of SMYD3 in nucleus was not changed.

doi:10.6342/NTU201602684

A

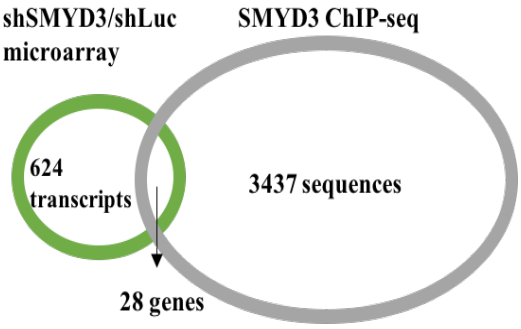

B

Symbol	Description	shSMYD3/shLuc
ANLN	Anillin, Actin Binding Protein	0.50
CYBRD1	Cytochrome B Reductase 1	0.33
DNMT3B	DNA (Cytosine-5-)-Methyltransferase 3 Beta	0.50
EFEMP1	EGF containing fibulin-like extracellular matrix protein 1	0.29
EXO1	exonuclease 1	0.47
FANCI	Fanconi anemia, complementation group I	0.47
GAD2	glutamate decarboxylase 2 (pancreatic islets and brain, 65kDa)	0.31
GALNT12	UDP-N-acetyl-alpha-D-galactosamine:polypeptide N-acetylgalactosaminyltransferase 12 (GalNAc-T12)	0.33
GMNN	geminin, DNA replication inhibitor	0.50
GPX2	glutathione peroxidase 2 (gastrointestinal)	0.35
IQGAP3	IQ motif containing GTPase activating protein 3	0.47
ITGA9	integrin, alpha 9	0.38
LRP1	low density lipoprotein receptor-related protein 1	0.44
MDC1	mediator of DNA-damage checkpoint 1	0.35
MYBL2	v-myb avian myeloblastosis viral oncogene homolog-like 2	0.38
NR5A2	nuclear receptor subfamily 5, group A, member 2	0.35
NT5C2	5'-nucleotidase, cytosolic II	0.50
OIP5	Opa interacting protein 5	0.47
POC1A	POC1 centriolar protein A	0.50
POLA2	polymerase (DNA directed), alpha 2, accessory subunit	0.47
POLQ	polymerase (DNA directed), theta	0.47
PRKAR2B	protein kinase, cAMP-dependent, regulatory, type II, beta	0.44
RAD54B	RAD54 homolog B (S. cerevisiae)	0.50
RET	ret proto-oncogene	0.44
SERPINA1	serpin peptidase inhibitor, clade A (alpha-1 antiproteinase, antitrypsin), member 1	0.29
SLC7A5	solute carrier family 7 (amino acid transporter light chain, L system), member 5	0.44
ST6GALNAC2	ST6 (alpha-N-acetyl-neuraminyl-2,3-beta-galactosyl-1,3)-N-acetylgalactosaminide alpha-2,6-sialyltransferase 2	0.41
TIAM1	T-cell lymphoma invasion and metastasis 1	0.50

C

Term	Genes	Count	p-value	Benjamini
DNA metabolic process	DNMT3B, FANCI, RAD54B, EXO1, MDC1, POLA2, POLQ	7	2.0E-4	7.6E-2
DNA repair	FANCI, RAD54B, EXO1, MDC1, POLQ	5	1.5E-3	2.5E-1
Cell cycle	FANCI, OIP5, RAD54B, ANLN, EXO1, GMNN, MDC1	7	1.9E-3	2.2E-1
Response to DNA damage stimulus	FANCI, RAD54B, EXO1, MDC1, POLQ	5	3.9E-3	3.2E-1
Cellular response to stress	FANCI, RAD54B, EXO1, MDC1, POLQ	5	1.7E-2	7.3E-1
M phase	OIP5, RAD54B, ANLN, EXO1	4	2.0E-2	7.3E-1

doi:10.6342/NTU201602684

Supplementary Fig1. Analysis of microarray and ChIP-seq data. (A) 28 genes were implicitly regulated by SMYD3 in microarray and ChIP-seq. (B) The relative expression fold of 28 genes after depletion of SMYD3 was listed. (C) The 28 genes were analyzed in The Database for Annotation, Visualization and Integrated Discovery (DAVID) and classified by gene ontology (GO) terms.

doi:10.6342/NTU201602684

Supplementary Fig 2. Predict transcription factor binding sites by PROMO.

The transcription factor binding sites on promoter (-1000 bp) of *MDC1, EXO1, and RAD54B* were analyzed by PROMO MultiSearch Promoter Sites. The analysis was restricted in transcription factors and transcription factor binding sites in human. The parameters were 100% similarity in all sequences. After analysis, there are transcription factor binding sites of C/EBPβ, glucocorticoid receptor, YY1, estrogen receptor, TFIID and XBP-1 on promoter of *MDC1, EXO1, and RAD54B.*

doi:10.6342/NTU201602684

CONTRIBUTION TABLE

Pin-Yu Wang	Fig. 1B, Fig. 2~4, Fig. 6A/C/D, Fig. 7, Fig. 10~11, Supplementary Fig. 2
Yun-Ju Chen	Fig. 1A, Fig. 5, Fig. 9, Supplementary Fig. 1
Cheng-Hui Tsai	Fig. 6A/B/C, Fig. 7

doi:10.6342/NTU201602684

REFERENCES

Albert, M., and Helin, K. (2010). Histone methyltransferases in cancer. Semin Cell Dev Biol *21*, 209-220.

Bekker-Jensen, S., Lukas, C., Melander, F., Bartek, J., and Lukas, J. (2005). Dynamic assembly and sustained retention of 53BP1 at the sites of DNA damage are controlled by Mdc1/NFBD1. J Cell Biol *170*, 201-211.

Bishop, A.J.R., and Schiestl, R.H. (2002). Homologous Recombination and Its Role in Carcinogenesis. Journal of Biomedicine and Biotechnology *2:2*, 75–85.

Cebria, F., Kobayashi, C., Umesono, Y., Nakazawa, M., Mineta, K., Ikeo, K., Gojobori, T., Itoh, M., Taira, M., Sanchez Alvarado, A., *et al.* (2002). FGFR-related gene nou-darake restricts brain tissues to the head region of planarians. Nature *419*, 620-624.

Chapman, J.R., and Jackson, S.P. (2008). Phospho-dependent interactions between NBS1 and MDC1 mediate chromatin retention of the MRN complex at sites of DNA damage. EMBO Rep *9*, 795-801.

Choudhury, A.D., Xu, H., and Baer, R. (2004). Ubiquitination and proteasomal degradation of the BRCA1 tumor suppressor is regulated during cell cycle progression. J Biol Chem *279*, 33909-33918.

Cock-Rada, A.M., Medjkane, S., Janski, N., Yousfi, N., Perichon, M., Chaussepied, M., Chluba, J., Langsley, G., and Weitzman, J.B. (2012). SMYD3 promotes cancer invasion by epigenetic upregulation of the metalloproteinase MMP-9. Cancer Res *72*, 810-820.

Dome`nec Farre´, Roma` Roset, Mario Huerta, Jose´ E. Adsuara, Llorenc¸ Rosello´, M. Mar Alba` , and Messeguer, X. (2003). Identification of patterns in biological sequences at the ALGGEN server PROMO and MALGEN. Nucleic Acids Research *31*, 3651-3653.

Escribano-Diaz, C., Orthwein, A., Fradet-Turcotte, A., Xing, M., Young, J.T., Tkac, J., Cook, M.A., Rosebrock, A.P., Munro, M., Canny, M.D., *et al.* (2013). A cell cycle-dependent regulatory circuit composed of 53BP1-RIF1 and BRCA1-CtIP controls DNA repair pathway choice. Mol Cell *49*, 872-883.

Foreman, K.W., Brown, M., Park, F., Emtage, S., Harriss, J., Das, C., Zhu, L., Crew, A., Arnold, L., Shaaban, S., *et al.* (2011). Structural and functional profiling of the human histone methyltransferase SMYD3. PLoS One *6*, e22290.

Hamamoto, R., Furukawa, Y., Morita, M., Iimura, Y., Silva, F.P., Li, M., Yagyu, R., and Nakamura, Y. (2004). SMYD3 encodes a histone methyltransferase involved in the proliferation of cancer cells. Nat Cell Biol *6*, 731-740.

Hamamoto, R., Silva, F.P., Tsuge, M., Nishidate, T., Katagiri, T., Nakamura, Y., and Furukawa, Y. (2006). Enhanced SMYD3 expression is essential for the growth of breast cancer cells. Cancer Sci *97*, 113-118.

Heyer, W.D., Ehmsen, K.T., and Liu, J. (2010). Regulation of homologous recombination in eukaryotes. Annu Rev Genet *44*, 113-139.

Huen, M.S., and Chen, J. (2008). The DNA damage response pathways: at the crossroad of protein modifications. Cell Res *18*, 8-16.

Hunt, C.R., Ramnarain, D., Horikoshi, N., Iyengar, P., Pandita, R.K., Shay, J.W., and Pandita, T.K. (2013). Histone modifications and DNA double-strand break repair after exposure to ionizing radiations. Radiat Res *179*, 383-392.

Kim, H., Heo, K., Kim, J.H., Kim, K., Choi, J., and An, W. (2009). Requirement of

doi:10.6342/NTU201602684

histone methyltransferase SMYD3 for estrogen receptor-mediated transcription. J Biol Chem *284*, 19867-19877.
Kim, J.M., Kim, K., Schmidt, T., Punj, V., Tucker, H., Rice, J.C., Ulmer, T.S., and An, W. (2015). Cooperation between SMYD3 and PC4 drives a distinct transcriptional program in cancer cells. Nucleic Acids Res *43*, 8868-8883.
Kolas NK, Chapman JR, Nakada S, Y.J., Chahwan R, Sweeney FD, Panier S, Mendez M, Wildenhain J, Thomson TM, Pelletier L, *et al.* (2007). Orchestration of the DNA-Damage Response by the RNF8 Ubiquitin Ligase. Science *318(5856)*, 1637-1640.
Kunizaki, M., Hamamoto, R., Silva, F.P., Yamaguchi, K., Nagayasu, T., Shibuya, M., Nakamura, Y., and Furukawa, Y. (2007). The lysine 831 of vascular endothelial growth factor receptor 1 is a novel target of methylation by SMYD3. Cancer Res *67*, 10759-10765.
Liu, C., Fang, X., Ge, Z., Jalink, M., Kyo, S., Bjorkholm, M., Gruber, A., Sjoberg, J., and Xu, D. (2007). The telomerase reverse transcriptase (hTERT) gene is a direct target of the histone methyltransferase SMYD3. Cancer Res *67*, 2626-2631.
Mailand, N., Bekker-Jensen, S., Faustrup, H., Melander, F., Bartek, J., Lukas, C., and Lukas, J. (2007). RNF8 ubiquitylates histones at DNA double-strand breaks and promotes assembly of repair proteins. Cell *131*, 887-900.
Martin, C., and Zhang, Y. (2005). The diverse functions of histone lysine methylation. Nat Rev Mol Cell Biol *6*, 838-849.
Mason, J.M., Dusad, K., Wright, W.D., Grubb, J., Budke, B., Heyer, W.D., Connell, P.P., Weichselbaum, R.R., and Bishop, D.K. (2015). RAD54 family translocases counter genotoxic effects of RAD51 in human tumor cells. Nucleic Acids Res *43*, 3180-3196.
Mattiroli, F., Vissers, J.H., van Dijk, W.J., Ikpa, P., Citterio, E., Vermeulen, W., Marteijn, J.A., and Sixma, T.K. (2012). RNF168 ubiquitinates K13-15 on H2A/H2AX to drive DNA damage signaling. Cell *150*, 1182-1195.
Mazur, P.K., Reynoird, N., Khatri, P., Jansen, P.W., Wilkinson, A.W., Liu, S., Barbash, O., Van Aller, G.S., Huddleston, M., Dhanak, D., *et al.* (2014). SMYD3 links lysine methylation of MAP3K2 to Ras-driven cancer. Nature *510*, 283-287.
Minter-Dykhouse, K., Ward, I., Huen, M.S., Chen, J., and Lou, Z. (2008). Distinct versus overlapping functions of MDC1 and 53BP1 in DNA damage response and tumorigenesis. J Cell Biol *181*, 727-735.
Nimonkar AV, O.A., Genschel J, Modrich P, Kowalczykowski SC (2008). Human exonuclease 1 and BLM helicase interact to resect DNA and initiate DNA repair. Proc Natl Acad Sci U S A *105(44)*, 16906-16911.
Panier, S., and Boulton, S.J. (2014). Double-strand break repair: 53BP1 comes into focus. Nat Rev Mol Cell Biol *15*, 7-18.
Pierce, A.J., Johnson, R.D., Thompson, L.H., and Jasin, M. (1999). XRCC3 promotes homology-directed repair of DNA damage in mammalian cells. GENES & DEVELOPMENT *13(20)*, 2633-2638.
Podhorecka, M., Skladanowski, A., and Bozko, P. (2010). H2AX Phosphorylation: Its Role in DNA Damage Response and Cancer Therapy. J Nucleic Acids *2010*.
Robert J. Sims 3rd, and Reinberg, D. (2004). From chromatin to cancer a new histone lysine methyltransferase enters the mix. Nature Cell Biology *6*, 685-687.
Sartori, A.A., Lukas, C., Coates, J., Mistrik, M., Fu, S., Bartek, J., Baer, R., Lukas, J., and Jackson, S.P. (2007). Human CtIP promotes DNA end resection. Nature *450*, 509-514.
Shi, W., Ma, Z., Willers, H., Akhtar, K., Scott, S.P., Zhang, J., Powell, S., and Zhang, J.

doi:10.6342/NTU201602684

(2008). Disassembly of MDC1 foci is controlled by ubiquitin-proteasome-dependent degradation. J Biol Chem *283*, 31608-31616.
Shun-Fu Tseng, Chun-Yu Chang, Kou-Juey Wu, and Teng, S.-C. (2005). Importin KPNA2 Is Required for Proper Nuclear Localization and Multiple Functions of NBS1. The Journal of Biological Chemistry *280*, 39594-39600.
Stucki, M., Clapperton, J.A., Mohammad, D., Yaffe, M.B., Smerdon, S.J., and Jackson, S.P. (2005). MDC1 directly binds phosphorylated histone H2AX to regulate cellular responses to DNA double-strand breaks. Cell *123*, 1213-1226.
Stucki, M., and Jackson, S.P. (2004). MDC1/NFBD1: a key regulator of the DNA damage response in higher eukaryotes. DNA Repair (Amst) *3*, 953-957.
Symington, L.S., and Gautier, J. (2011). Double-strand break end resection and repair pathway choice. Annu Rev Genet *45*, 247-271.
Thorslund, T., McIlwraith, M.J., Compton, S.A., Lekomtsev, S., Petronczki, M., Griffith, J.D., and West, S.C. (2010). The breast cancer tumor suppressor BRCA2 promotes the specific targeting of RAD51 to single-stranded DNA. Nat Struct Mol Biol *17*, 1263-1265.
Tomimatsu, N., Mukherjee, B., Catherine Hardebeck, M., Ilcheva, M., Vanessa Camacho, C., Louise Harris, J., Porteus, M., Llorente, B., Khanna, K.K., and Burma, S. (2014). Phosphorylation of EXO1 by CDKs 1 and 2 regulates DNA end resection and repair pathway choice. Nat Commun *5*, 3561.
Tran, P.T., Erdeniz, N., Symington, L.S., and Liskay, R.M. (2004). EXO1-A multi-tasking eukaryotic nuclease. DNA Repair (Amst) *3*, 1549-1559.
Van Aller, G.S., Reynoird, N., Barbash, O., Huddleston, M., Liu, S., Zmoos, A.F., McDevitt, P., Sinnamon, R., Le, B., Mas, G., *et al.* (2012). Smyd3 regulates cancer cell phenotypes and catalyzes histone H4 lysine 5 methylation. Epigenetics *7*, 340-343.
Wilson, K.A., and Stern, D.F. (2008). NFBD1/MDC1, 53BP1 and BRCA1 have both redundant and unique roles in the ATM pathway. Cell Cycle *7*, 3584-3594.
Zhang, J., Ma, Z., Treszezamsky, A., and Powell, S.N. (2005). MDC1 interacts with Rad51 and facilitates homologous recombination. Nat Struct Mol Biol *12*, 902-909.
Zhenkun Lou, Claudia Christiano Silva Chini, Katherine Minter-Dykhouse, and Chen, J. (2003a). MDC1 Regulates BRCA1 Localization and Phosphorylation in DNA Damage Checkpoint Control. J Biol Chem *278(16)*, 13599-13602.
Zhenkun Lou, Claudia Christiano Silva Chini, Katherine Minter-Dykhouse, and Chen, J. (2003b). Mediator of DNA damage checkpoint protein 1 regulates BRCA1 localization and phosphorylation in DNA damage checkpoint control. J Biol Chem *278*, 13599-13602.
Zou, J.N., Wang, S.Z., Yang, J.S., Luo, X.G., Xie, J.H., and Xi, T. (2009). Knockdown of SMYD3 by RNA interference down-regulates c-Met expression and inhibits cells migration and invasion induced by HGF. Cancer Lett *280*, 78-85.

doi:10.6342/NTU201602684